Available online at www.sciencedirect.com
SCIENCE DIRECT®
Journal of Power Sources 126 (2004) 175–181
JOURNAL OF POWER SOURCES
www.elsevier.com/locate/jpowsour

Influence of electroformation charge capacity on the mechanism of charge/discharge process for positive electrode in lead–acid cells

Jan M. Skowroński [a,b,*], Tomasz Doczekalski [b]

[a] *Poznań University of Technology, Institute of Chemistry and Technical Electrochemistry, ul. Piotrowo 3, 60-965 Poznań, Poland*
[b] *Central Laboratory of Batteries and Cells, ul. Forteczna 12/14, 61-362 Poznań, Poland*

Received 3 October 2002; received in revised form 4 September 2003; accepted 8 September 2003

Abstract

The aim of the present paper was to determine the electrochemical state of the positive electrodes during the formation process using the electrochemical impedance spectroscopy (EIS) and cyclic voltammetry (CV). The investigations of typical positive electrodes were carried out for 12 states-of-electroformation (SOE). It was found that during electroformation the positive electrodes undergo dramatic changes which are reflected in EIS spectra. SOE strongly influences the equivalent electrical circuit and the range of impedance spectrum of non-inductive character. The obtained results showed that EIS technique can be used as a sensitive method allowing to distinguish the consecutive steps of electroformation. The conclusions drawn from EIS measurements are confirmed by CV measurements performed for selected SOEs.
© 2003 Elsevier B.V. All rights reserved.

Keywords: Lead–acid cell; Positive electrode; Electroformation; Impedance spectroscopy; Cyclic voltammetry

1. Introduction

The electroformation process is the last step in the lead–acid battery manufacturing. The standard methods employed to control this process are based on the measurements of the following parameters:

- electrolyte density,
- temperature of cells,
- amount of charge accumulated,
- cell voltage.

The above parameters allow neither the indication of the completion of electroformation nor the estimation of the amount of lead dioxide generated.

Hughes et al. [1] carried out the electrochemical impedance spectroscopy (EIS) measurements for two batches of lead–acid cells, involving the freshly produced cells and those which worked for 5 years. The authors revealed essential differences in EIS spectra recorded for batteries belonging to each set. In the next paper [2], they pointed out that the value of ohmic resistance is useful for determining the state-of-charge (SOC) because this parameter directly relates to specific gravity of electrolyte. Böttcher and Panesar [3] presented the impedance model of PbO_2 electrode as a complex system composed of four subsystems connected in series. Jinda et al. [4] characterized lead–acid cells using EIS method during galvanostatic charging. They showed that during the first half of the charging period the impedance of cell is controlled by the positive electrode whereas on further run the kinetics of charging depends on the processes occurring at negative electrodes. Viswanathan et al. [5] investigated typical lead–acid cells (4 V, 3 Ah; 4 V, 9 Ah; 6 V, 6.5 Ah) and observed that ohmic resistance decreased as SOC increased. From the analysis of equivalent electrical circuit they concluded that capacitance of double layer and SOC increases in parallel. In 1998, Huet [6] reviewed the practical application of EIS for determining both SOC and the state-of-health (SOH) in secondary cells. The conclusion was that the determination of SOC and SOH for lead–acid cells by EIS should be performed in the high frequency range from 10 to 100 Hz. Karden et al. [7] used EIS method for characterization and modeling the industrial batteries. EIS measurements carried out for cells and half-cells have shown that the results are reproducible and provide information about the processes occurring inside lead–acid battery. Hammouche et al. [8] investigated the oxygen and hydrogen evolution reaction in flooded lead–acid batteries by EIS technique. Based on the results obtained, the authors concluded that gassing processes proceeding in lead–acid

* Corresponding author. Tel.: +48-61-665-3641; fax: +48-61-665-2571.
E-mail address: jan.skowronski@put.poznan.pl (J.M. Skowroński).

0378-7753/$ – see front matter © 2003 Elsevier B.V. All rights reserved.
doi:10.1016/j.jpowsour.2003.09.036

battery can be distinguished by EIS in the frequency range 2–0.005 mHz. Salkind et al. [9] used EIS method to examine small valve regulated lead–acid batteries (VRLA). The objective of this work was to characterize VRLA batteries at different SOC. The authors concluded that SOC can be described by EIS data. Examining the discharge mechanism of active material of the positive electrode by EIS method, Pavlov and Petkova [10,11] assigned two equivalent electrical circuits, described by codes $R(Q[RQ])$ and $R(RQ)(Q[RQ])$, to charged and discharged state of positive electrode, respectively. The authors showed that elements of the equivalent circuits changing during cycling, such as R_{ct} (charge-transfer resistance), R_i (resistance of interface), R_Ω (ohmic resistance) and R_{diff} (resistance of diffusion), are useful in determining SOH and make the indication of the state of positive electrode near the end of life possible.

After considering the reports mentioned above, we decided to use EIS method to examine the electroformation process of positive electrodes of lead–acid cell. The EIS measurements were carried out to control the state-of-electroformation (SOE). The main objective of this work was to estimate the characteristic parameters of the impedance spectra and/or the equivalent electrical circuits in relation to SOE. SOE was divided into 12 time intervals of charging selected based on the potential profile of electrode.

2. Experimental

The raw materials, lead powder from Barton's pot and lead alloys, used for manufacturing the grids casting were received from AUTOPART-Mielec (the Polish producer of starter batteries). The positive electrodes (the working electrodes) were prepared by pasting positive active material (made by mixing 2000 g of lead oxide powder, 270 cm^3 of water and 160 cm^3 of H_2SO_4 with specific gravity 1.4 g/cm^3) onto grids made of Pb–1.3Sb alloy. Upon curing in air (45 °C, 98% relative humidity), $3PbO{\cdot}PbSO_4{\cdot}H_2O$ (3BS) was formed. Then one positive electrode was vertically placed between two negative electrodes made of the same alloy and the set of electrodes was then put into the box filled with sulfuric acid solution (1.25 g/cm^3). The capacity of experimental cell was 2 Ah. Because the charge limiting electrode was the positive electrode, its capacity was recognized as identical to the complete cell. After 1 h of soaking, the electrodes in the experimental cells were subjected to the electroformation process with current density 3 mA/cm^2 for 50 h.

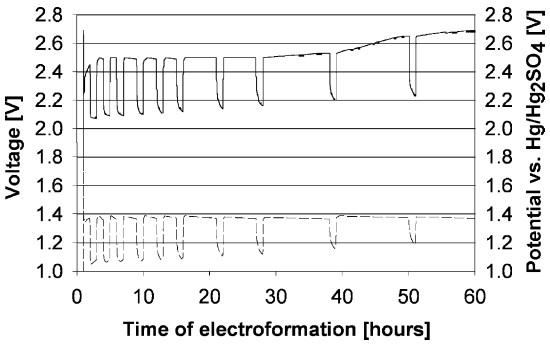

Fig. 1. Potential-time (dashed line) and voltage-time (solid line) characteristics recorded during electrofomation of positive electrode and lead–acid cell, respectively.

Based on the literature data [12–14], the period of electroformation was divided into the time intervals depending on the processes expected to occur on positive electrode. At the beginning of the process, involving the chemical and electrochemical reactions taking place in parallel, the time intervals were 1–2 h. Next, two intervals were expanded to 5 h. Assuming that the changes in chemistry and electrochemistry of positive electrode proceed slower for advanced SOE, the last three time intervals were twice prolonged.

EIS measurements (in the frequency range 10 mHz–60 kHz with ac voltage amplitude ±5 mV) were performed in a three-electrode arrangement for the positive electrodes (52 mm × 42 mm × 2 mm). The impedance spectra were recorded at the given steps of electroformation (Table 1). Using a three-electrode system, the positive electrode (the working electrode) was sandwiched between two negative electrodes (the counter electrode) and the $Hg/Hg_2SO_4/1\,M\ H_2SO_4$ reference electrode was placed in the electrolytic cell at vicinity to the positive electrode. After the time when electroformation was reached the charge current was cut off for 30 min and the potential of electrode was allowed to drop until the stable value was attained and then EIS measurements were started (see Fig. 1). EIS measurements were performed using the Solartron 1260 impedance analyzer coupled with the PAR 273A potentiostat–galvanostat. For each impedance spectrum, the equivalent electrical circuit was calculated. Frequency response analyzer software (FRA 2.4) was used for fitting elements of equivalent circuit.

For description of the equivalent electrical circuits, the following symbols are used throughout the paper: R_Ω: ohmic resistance; C: double layer capacitance; $R_{ct1,2}$: charge transfer resistance; $Q_{dl1,2}$: constant phase element representing

Table 1
Stages of electroformation for positive electrode determined by EIS measurements in relation to the state-of-electroformation (SOE)

	1	2	3	4	5	6	7	8	9	10	11	12
Time of electroformation (h)	0	1	2	3	5	7	9	14	19	29	40	50
Capacity charged (Ah)	0	0.13	0.26	0.39	0.65	0.91	1.17	1.82	2.47	3.77	5.20	6.50
Positive electrode	Stage A								Stage B			
	Substage 1		Substage 2			**Substage 1**			Substage 2			

double layer capacitance; Q_{diff}: constant phase element representing the change of diffusion layer.

The cyclic voltammetry (CV) measurements of the positive electrodes (15 mm × 15 mm × 2 mm) were performed in sulfuric acid solutions (1.25 g/cm^3) in the potential range from +800 to +1750 mV using Autolab PSTAT-30 potentiostat–galvanostat. The measurements were performed for positive electrodes earlier galvanostatically oxidized during 2, 3, 5, 9 and 19 h of electroformation. CV measurements with a scan rate of 2 mV/s were performed in a three-electrode cell identical to that used for EIS measurements.

All electrochemical measurements were made at a temperature of 20 °C.

3. Results and discussion

3.1. Impedance measurements

The description codes of the equivalent electrical circuits and the values of fitting parameters are presented in Table 2. For the fitting procedure the region of non-inductive character was only taken from the impedance spectrum.In agreement with the mechanisms of electroformation for positive electrodes reported earlier [12–14], the process examined here is composed of two stages. The first stage occurring for 4 h is connected with the chemical reaction between H_2SO_4 and tet-PbO and the electrochemical reaction resulting in the formation of α- and partially β-PbO_2. During the second stage, lead sulfate is oxidized only to β-PbO_2 form. Papazov [14] reported that during the first stage of formation 85–90% of charge is consumed for the conversion of the active material of electrode and only 10–15% for gas evolution. During the second stage of formation the situation is opposite.

Pavlov et al. [12] using the electroformation current density of 5 mA/cm^2 attained the first stage of electroformation before 4 h and after this time the second stage developed. Because in the present paper, the electroformation current density was 3 mA/cm^2 (1.67 times lower) and taking into account that the thicknesses of working electrodes used by Pavlov et al. and by us were comparable, the first stage was attained by us before 7 h of electroformation (denoted as stage A in Table 1). Based on this, it is justified to assume

Table 2
Values of fitting parameters of equivalent circuits for impedance spectra recorded during electroformation of positive electrode

SOE	Description code	Non-inductive frequency range (Hz)	Values of fitting parameters			
1	$R_\Omega(R_{ct1}Q_{dl1})(R_{ct2}Q_{dl2})$	1423–0.01	$R_\Omega = 0.1739\,\Omega$ $R_{ct2} = 85.30\,\Omega$	$R_{ct1} = 12.45\,\Omega$ $Q_{dl2} = 0.1863 \times 10^{-2}$	$Q_{dl1} = 0.9605 \times 10^{-3}$ $n_{dl2} = 0.7630$	$n_{dl1} = 0.8793$
2	$R_\Omega(R_{ct1}Q_{dl1})(R_{ct2}Q_{dl2})$	1423–0.01	$R_\Omega = 0.1449\,\Omega$ $R_{ct2} = 6.44\,\Omega$	$R_{ct1} = 0.0548\,\Omega$ $Q_{dl2} = 8.099$	$Q_{dl1} = 4.428$ $n_{dl2} = 0.8738$	$n_{dl1} = 0.3991$
3	$R_\Omega(R_{ct1}Q_{dl1})(R_{ct2}Q_{dl2})$	1423–0.01	$R_\Omega = 0.1377\,\Omega$ $R_{ct2} = 7.4400\,\Omega$	$R_{ct1} = 0.0726\,\Omega$ $Q_{dl2} = 15.9600$	$Q_{dl1} = 30.75$ $n_{dl2} = 0.9053$	$n_{dl1} = 0.3180$
4	$R_\Omega(Q_{dl1}[R_{ct1}Q_{diff}])(R_{ct2}Q_{dl2})$	1423–0.01	$R_\Omega = 0.1439\,\Omega$ $Q_{diff} = 19.37$ $n_{dl2} = 0.8741$	$Q_{dl1} = 1.727$ $n_{diff} = 0.9567$	$n_{dl1} = 0.5093$ $R_{ct2} = 0.0231\,\Omega$	$R_{ct1} = 0.0397\,\Omega$ $Q_{dl2} = 25.64$
5	$R_\Omega(Q_{dl1}[R_{ct1}Q_{diff}])(R_{ct2}Q_{dl2})$	1067–0.01	$R_\Omega = 0.1438\,\Omega$ $Q_{diff} = 34.98$ $n_{d12} = 0.7742$	$Q_{dl1} = 3.085$ $n_{diff} = 0.9760$	$n_{dl1} = 0.5070$ $R_{ct2} = 0.0281\,\Omega$	$R_{ct1} = 0.0258\,\Omega$ $Q_{dl2} = 57.55$
6	$R_\Omega(R_{ct1}Q_{d12}])(R_{ct2}Q_{diff})$	1067–0.01	$R_\Omega = 0.1419\,\Omega$ $Q_{d12} = 1.512$ $n_{diff} = 0.8744$	$R_{ct1} = 0.0097\,\Omega$ $n_{dl2} = 0.5977$	$Q_{dl1} = 52.74$ $R_{ct2} = 0.0250\,\Omega$	$n_{dl1} = 0.9317$ $Q_{diff} = 66.31$
7	$R_\Omega(R_{ct1}Q_{dl1})(Q_{dl2}[R_{ct2}Q_{diff}])$	1067–0.01	$R_\Omega = 0.1423\,\Omega$ $Q_{d12} = 1.100$ $n_{diff} = 0.9284$	$R_{ct1} = 0.0127\,\Omega$ $n_{dl2} = 0.6575$	$Q_{dl1} = 100.4$ $R_{ct2} = 0.0217\,\Omega$	$n_{dl1} = 0.7718$ $Q_{diff} = 64.15$
8	$R_\Omega(R_{ct1}Q_{dl1})(Q_{dl2}[R_{ct2}Q_{diff}])$	800–0.01	$R_\Omega = 0.1412\,\Omega$ $Q_{d12} = 1.494$ $n_{diff} = 0.9502$	$R_{ct1} = 0.0187\,\Omega$ $n_{dl2} = 0.7434$	$Q_{dl1} = 202.9$ $R_{ct2} = 0.0116\,\Omega$	$n_{dl1} = 0.5702$ $Q_{diff} = 88.57$
9	$R_\Omega(R_{ct1}Q_{dl1})(Q_{dl2}[R_{ct2}Q_{diff}])$	600–0.01	$R_\Omega = 0.1356\,\Omega$ C = 29.83 F	$R_{ct1} = 0.0160\,\Omega$ $R_{ct2} = 0.0155\,\Omega$	$Q_{dl1} = 19.93$ $Q_{diff} = 125.3$	$n_{dl1} = 0.5666$ $n_{diff} = 0.8601$
10	$R_\Omega(R_{ct1}Q_{dl1})(C[R_{ct2}Q_{diff}])$	337–0.01	$R_\Omega = 0.1374\,\Omega$ C = 30.79 F	$R_{ct1} = 0.0134\,\Omega$ $R_{ct2} = 0.0135\,\Omega$	$Q_{dl1} = 15.38$ $Q_{diff} = 128.2$	$n_{dl1} = 0.6324$ $n_{diff} = 0.8960$
11	$R_\Omega(R_{ct1}Q_{dl1})(C[R_{ct2}Q_{diff}])$	337–0.01	$R_\Omega = 0.1352\,\Omega$ C = 16.42 F	$R_{ct1} = 0.0107\,\Omega$ $R_{ct2} = 0.0124\,\Omega$	$Q_{dl1} = 4.291$ $Q_{diff} = 224.4$	$n_{dl1} = 0.7670$ $n_{diff} = 0.7659$
12	$R_\Omega(R_{ct1}Q_{dl1})(C[R_{ct2}Q_{diff}])$	337–0.01	$R_\Omega = 0.1338\,\Omega$ C = 25.90 F	$R_{ct1} = 0.0114\,\Omega$ $R_{ct2} = 0.0134\,\Omega$	$Q_{dl1} = 8.975$ $Q_{diff} = 161.9$	$n_{dl1} = 0.6793$ $n_{diff} = 0.9256$

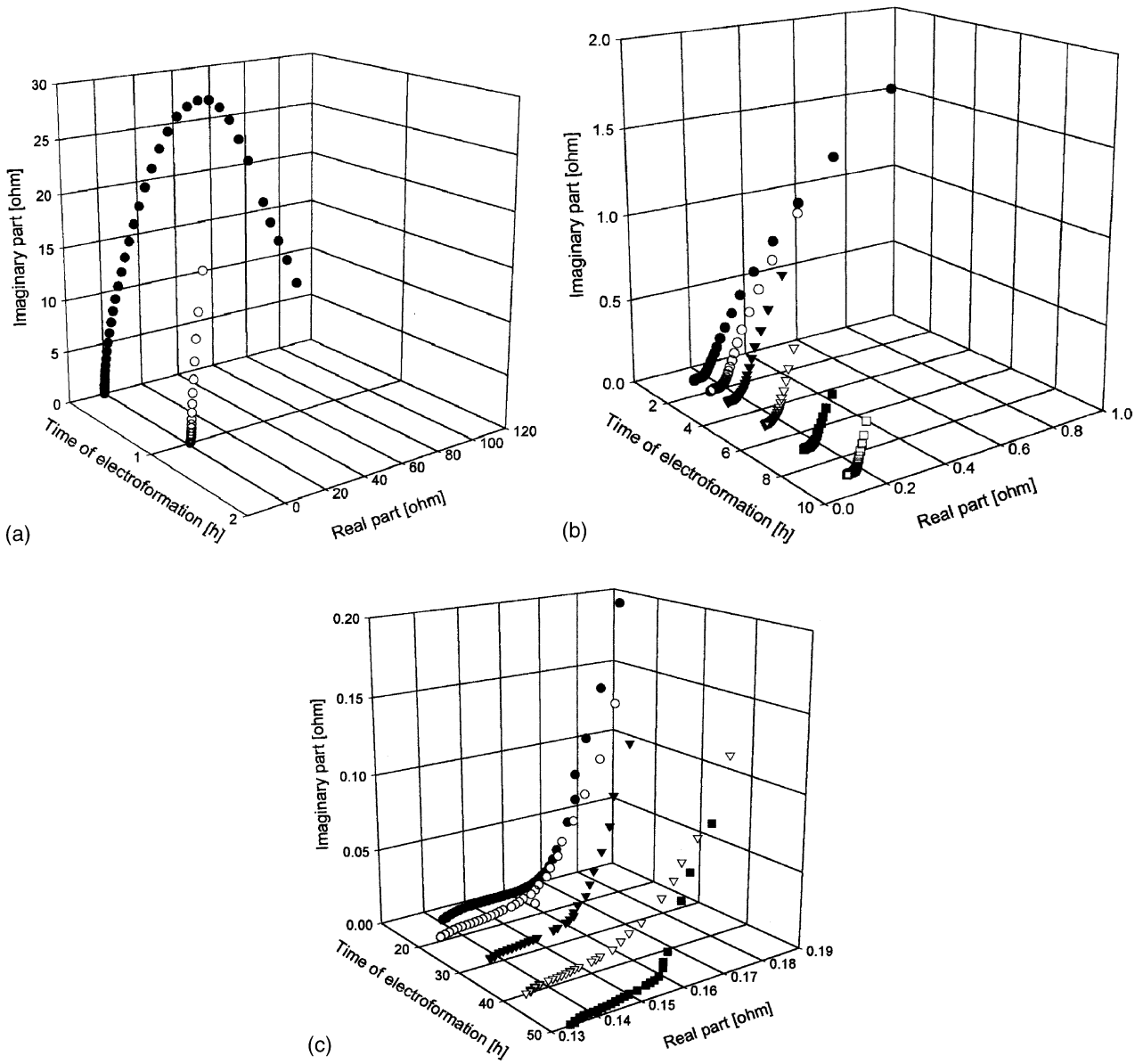

Fig. 2. Impedance spectra recorded during electroformation of positive-electrode of lead–acid cell. (a) After 1 h of soaking followed by 1 h of electroformation (*note*: for easier comparison of both spectra, the values of impedance spectrum recorded after 1 h were multiplied by 10); (b) for the periods of time ranging between 2 and 9 h; (c) for the periods of time ranging between 10 and 50 h.

that the first stage determined by Pavlov et al. [12] is the sum of substages A1 and A2 distinguished by us (see Table 1).

Impedance spectra recorded here for the positive electrodes during electroformation (Table 2, Fig. 2), can be described by four equivalent circuits dependent on the time of electroformation.

- $R_\Omega(R_{ct1}Q_{dl1})(R_{ct2}Q_{dl2})$: from 0 to 2 h (substage A1),

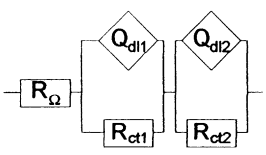

- $R_\Omega(Q_{dl1}[R_{ct1}Q_{diff}])(R_{ct2}Q_{dl2})$: from 3 to 5 h (substage A2),

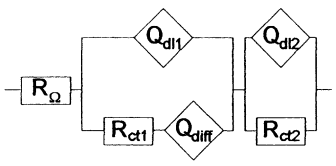

- $R_\Omega(R_{ct1}Q_{dl1})(Q_{dl2}[R_{ct2}Q_{diff}])$: from 7 to 14 h (substage B1),

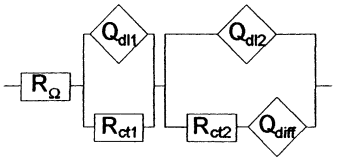

- $R_\Omega(R_{ct1}Q_{dl1})(C[R_{ct2}Q_{diff}])$: from 19 to 50 h; charged electrode (substage B2).

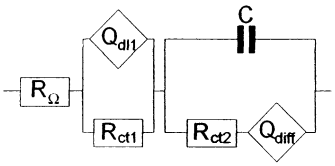

Each of the above equivalent circuits describing the separated substages of electroformation is composed of the ohmic resistance and two subcircuits of *RQ* in series. The number of individual subcircuits in the electrical circuit corresponds to the number of phases distinguished by EIS measurements.

The obtained sequence of equivalent circuits allows the assumption that the process of electroformation of the positive electrode proceeds through two stages (A and B). Concerning the above circuits for both stages, we distinguished two substages within each stage (substages A1 and A2 for the first stage and substages B1 and B2 for the second stage). Substage A1 is controlled by charge transfer and terminates after about 2 h (Fig. 2a and b). A small amount of charge passing through the electrode during the first hour of electroformation strongly contributes to the decrease in internal resistance R_{ct1} (Fig. 2a). As a consequence, the electric contact between grid and positive active material is improved which brings about the decrease in element R_{ct1} from 12.45 Ω for the electrode before starting the electroformation process to 0.073 Ω after 2 h of the process (Table 2).

After 3 h of electroformation the equivalent circuit matching the impedance spectrum changes to $R_\Omega(Q_{dl1}[R_{ct1}Q_{diff}])(R_{ct2}Q_{dl2})$ (substage A2) and the process becomes controlled by diffusion described by element Q_{diff}. The shape of impedance spectrum changes considerably and element Q_{diff} associated with diffusion appears. This parameter may be ascribed to the diffusion of ions inside the porous electrode of PbO_2. The formation of PbO_2 within the active material of electrode starts at the grid of electrode and shifts in the direction of electrolyte. Because the formation of PbO_2 is faster and faster as electric contact between grid and lead oxide is improved, the diffusion rate of sulfuric acid controls the conversion of PbO and 3BS to PbO_2. The mechanism proposed here for substages A1 and A2 of electroformation is consistent with the model of impedance spectrum reported by Mauracher and Karden [15]. According to this model, the impedance spectra recorded in the frequency range 100–10 mHz correspond to the process controlled by diffusion inside the porous material.

The third substage (B1) begins after 7 h of electroformation and endures up to 14 h. Impedance spectra recorded for this substage of electroformation as well as the relevant equivalent circuit indicates that the reaction system is still composed of three interfaces: grid/PbO_2, PbO_2/$PbSO_4$ and $PbSO_4$/electrolyte. However, as seen from comparison of the equivalent circuits for substages A2 and B1, element Q_{diff} in the latter circuit displaces from the interface grid/PbO_2 to PbO_2/$PbSO_4$. It means that the reaction phase moves to the outer regions of electrode. Such a system is in accordance with the structure of the electrolyte/PbO_2 interface proposed and described by Böttcher and Panesar [3]. For this stage of electroformation, the process is still controlled by diffusion (the value of element Q_{diff} for which $n = 0.60$ is close to the Wartburg diffusion) and proceeds in the inner regions of porous structure of active material. The values of capacitance parameters of equivalent circuit increase step by step as the time of electroformation increases.

The last substage of electroformation (B2) starting for the period of time longer than 19 h of charging, is associated with the formation of PbO_2 near the electrode–electrolyte interface. The equivalent circuits corresponding to this as well as to the next steps of electroformation indicates that the reaction system is similar to the previous one but the elements of equivalent circuits describing the electrochemical state of the positive electrodes undergo to the ideal capacitance. After storing enough amount of charge the composition of the positive active material becomes homogenous and electrochemical reaction comprises the bulk of electrode. As a consequence, constant phase element Q_{dl2} in the equivalent circuit for substage B1 turns into element C (double layer capacitance) for substage B2. It indicates that the oxidation of $PbSO_4$ into PbO_2 is preceded by charging the double layer at the electrode/electrolyte interface.

At present, a simple comparison of the calculated values of the circuit elements for positive electrodes is very difficult. During electroformation, the positive electrodes of lead–acid cell undergo complex electrochemical changes involving the grid corrosion, the formation of α- and β-PbO_2, the diffusion of electrolyte, etc. After soaking the electrode, the reaction system is composed of three components (grid, PbO + 3BS, electrolyte) and two interfaces: grid/(PbO + 3BS) and (PbO + 3BS)/electrolyte while the successive charging changes the electrochemical system into grid/PbO_2/PbO_n/electrolyte ($1 < n < 2$). Such an electrode system is consistent with that reported by Pavlov et al. [10,11,16], where electrode grid is interconnected with the positive active material by corrosion layer formed on the grid surface. The investigated effects arise not only from the surface regions of electrode but also from its interior. For all the stages of the electroformation process only element R_Ω corresponds to the same element of electrode while the other elements of equivalent circuit describe the regions of electrochemical reaction. These regions move along with PbO_2 formation. For example, the value of element Q_{dl1} after 5 and 7 h of electroformation changed from 239 to 52.74 (Table 2). A similar situation was after 14 and 19 h of the process. Moreover, it was found that the non-inductive range of frequencies was conditional on states of electroformation. Owing to this, the limit of high frequency with non-inductive character can be used as sensitive indicator of SOE (Table 2).

The equivalent circuit for the positive electrode after 50 h of electroformation ($R_\Omega(R_{ct1}Q_{dl1})(C[R_{ct2}Q_{diff}])$ is not the

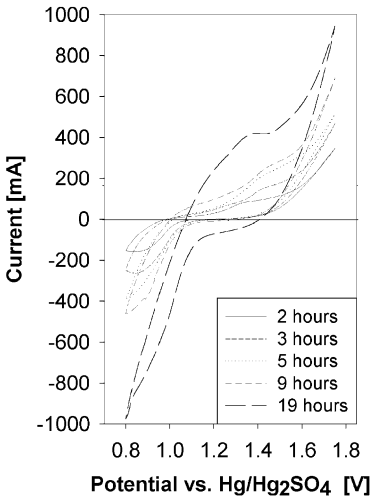

Fig. 3. Cyclic voltammograms (the second cycles) recorded for positive electrodes after different hours of electroformation (scan rate: 2 mV/s).

same (two-phase system) as that for fully charged positive electrodes ($R_\Omega(Q_{dl}[R_{ct}Q_{diff}])$ reported by Pavlov and Petkova [11]. One of the reasons for this discrepancy is that our electrodes were not subjected to the charge/discharge cycling, which makes the complete transformation of the starting $PbSO_4$ electrode materials into PbO_2 easier.

3.2. CV measurements

The cyclic voltammetric measurements were performed for positive electrodes oxidized earlier for various times of electroformation. As can be seen in Fig. 3, CV curves well reflect the changes in the kinetics of redox reactions depending on the stage of electroformation evaluated from EIS data. The susceptibility of electrode to oxidation is higher for electrodes representing higher stage of electroformation. CV curve for electrode electroformed only 2 h (substage A1) exhibits the lowest anodic charge. On comparing the electrodes electroformed for 2 and 3 h, the lower anodic charge and current plateau in the potential range 1.35–1.55 V observed for the electrode after 2 h of electroformation may be related to the impeded charge transfer resulting from hindrances remaining at the grid/(PbO+3BS) interface. During the backward scan, the passive layer existing on the electrode grid makes the recovery of charge difficult followed by the cathodic reduction starting at the highest overpotential. It corresponds to the lowest potential of 1.20 V at which the curve pass to the negative side of the CV plot (Table 3). The anodic charge and the charge/discharge reversibility are improved for electrode electroformed 1 h longer (substage A2; curve for 3 h in Fig. 3). Based on the impedance data listed in Table 2, such an improvement may be attributed to the change in the mechanism of reaction. Due to the formation of PbO_2 on the surface of grid, the resistance of charge transfer at the grid/PbO_2 boundary decreases markedly bringing about the displacement of the oxidized substance from the inner to outer regions of electrode. For this electrode (attaining substage A2), the kinetics of reaction is governed by diffusion of sulfuric acid into the porous structure of electrode. The character of CV curve after 5 h of electroformation is generally identical to electrode oxidized for 3 h. The only difference is the increased anodic and cathodic charges resulting from higher anodic charge accumulated in the electrode during longer electroformation (note that the second cycles are shown in Fig. 3). CV curve for electrode electroformed for 9 h (substage B1) is noticeably different in comparison with electrodes oxidized for 5 and 7 h. The higher total anodic charge is quite understandable because of longer time of electroformation. More interesting is, however, the fact that the increase in total anodic charge is greatly contributed by the process occurring at lower potentials between 1.0 and 1.3 V (two anodic peaks are well observed). Such a behavior corroborates the conclusions drawn from EIS measurements. As mentioned in Section 3.1, for substage B1 of electroformation the oxidation of $PbSO_4$ to PbO_2 occurs on PbO_2-covered surface of grid as well as in the bulk of electrode. The change in the equivalent circuits on going from substage B1 to B2 is distinctly reflected on CV curve recorded for electrode oxidized for 19 h (substage B2). During the forward scan, the anodic current increases abruptly at the potential of about 1.0 V and forms a well shaped peak at 1.37 V. Such a behavior is in accordance with the prediction based on EIS data and can be attributed to the reaction involving the whole of electrode. Among all the examined electrodes, this electrode gains the highest anodic charge and the process of electroreduction starts to occur at the highest potential of 1.41 V after the polarization direction is changed. The discharge of electrode continues down to the potential of 1.1 V and then accelerates rapidly. The highest charge is regained but it is worthy of noting that the cathodic process is not yet terminated at the reversion potential of 0.8 V. Despite this, it is clear from CV curves that the charge/discharge process for this electrode occurs at the narrowest range of potential.

Table 3
The values of potential corresponding to the positive-negative current change during the backward scan (see Fig. 3)

Time of electroformation (h)	Potential (V)
2	1.202
3	1.239
5	1.252
9	1.313
19	1.410

4. Conclusions

The electrochemical impedance spectroscopy coupled with cyclic voltammetry appeared to be useful tool for evaluation of the electrochemical state of the positive electrodes during the formation process. Based on EIS data, it was shown that the state-of-electroformation (SOE) can

be described by the equivalent electrical circuits containing the following elements: R_Ω (ohmic resistance), C (double layer capacitance), $R_{ct1,2}$ (charge transfer resistance), $Q_{dl1,2}$ (constant phase element representing double layer capacitance), Q_{diff} (constant phase element representing the change of diffusion layer). It was found that the limit of high frequency of non-inductive character can also be used as a sensitive indicator of SOE.

Considering 12 SOEs dependent on the time of charging, for the process of electroformation two essential stages (denoted A and B), associated with different chemical and electrochemical properties of the oxidized electrode material, were recognized. However, the analysis of EIS data obtained for electrodes oxidized during purposely fixed periods of electroformation allowed us to distinguish two substages within each of the stage. The first substage (A1) occurring at the beginning of the process is controlled by charge transfer and terminates after about 2 h. In this period of time, the internal resistance R_{ct1} decreases giving rise to the improvement of the electric contact between grid and the positive active material. After 3 h of electroformation (substage A2), the process changes to be controlled by the diffusion of ions inside the porous electrode of PbO_2 (described by element Q_{diff}). The formation of PbO_2 within the active material of electrode starts at the grid of electrode and moves in the direction of electrolyte. In this substage, the process involves two interfaces (grid/PbO_2 and PbO_2/PbO + 3BS) and the diffusion rate of sulfuric acid controls the conversion of PbO + 3BS to PbO_2. Substage B1 (lasting 7–14 h) still consists of the two interfaces, but element Q_{diff} in the equivalent circuit obtained in this substage displaces from the interface grid/PbO_2 to PbO_2/$PbSO_4$. This feature indicates that the reaction phase moves to the outer regions of electrode. During the last substage of electroformation (B2), starting at 19 h of charging, the formation of PbO_2 near the electrode–electrolyte interface develops.

The model of electroformation proposed based on EIS measurements was supported by CV measurements made for electrodes earlier oxidized for such time intervals to attain all the substages of electroformation. It was shown that the hindrances in the kinetics of redox reactions are the most pronounced for electrode prepared in substage A1. The situation changes for the better for electrode reaching substage A2, for which the increase in both the anodic charge and the charge/discharge reversibility is noted. Distinct changes in character of CV curve are observed for electrode oxidized for 9 h (substage B1). In this case, the anodic charge markedly increases, the oxidation process starts at lower potential and the reduction process is initiated at higher potential as compared to electrodes electroformed in substages A1 and A2. The electrode representing substage B2 provides CV curves demonstrating strongly highest charge and discharge capacities. The oxidation process for this electrode starts very steeply at the lowest potential, whereas the reduction process occurs with the lowest overpotential.

References

[1] M. Hughes, R.T. Barton, S.A.G.R. Karunathilaka, N.A. Hampson, R. Leek, J. Power Sources 17 (1986) 305.
[2] R.T. Barton, P.J. Mitchell, J. Power Sources 27 (1989) 287.
[3] F. Böttcher, H.S. Panesar, J. Power Sources 36 (1991) 439.
[4] J. Jinda, M. Musilova, J. Mrha, A.A. Taganova, J. Power Sources 37 (1992) 403.
[5] V.V. Viswanathan, A.J. Salkind, J.J. Kelley, J.B. Ockerman, J. Appl. Electrochem. 25 (1995) 729.
[6] F. Huet, J. Power Sources 70 (1998) 59.
[7] E. Karden, S. Buller, R.W. Doncker, J. Power Sources 85 (2000) 72.
[8] A. Hammouche, E. Karden, J. Walter, R.W. Doncker, J. Power Sources 96 (2001) 106.
[9] A. Salkind, T. Atwater, P. Singh, S. Nelatury, S. Damodar, C. Fennie Jr., D. Reisner, J. Power Sources 96 (2001) 151.
[10] D. Pavlov, G. Petkova, J. Electrochem. Soc. 149 (2002) A644.
[11] D. Pavlov, G. Petkova, J. Electrochem. Soc. 149 (2002) A654.
[12] D. Pavlov, G. Papazov, V. Iliev, J. Electrochem. Soc. 119 (1972) 8.
[13] L. Zerroual, F. Tedjar, J. Power Sources 41 (1993) 231.
[14] G. Papazov, in: Proceedings of the LABAT Conference, Varna, 1993 (extended abstract no. 40).
[15] P. Mauracher, Karden, J. Power Sources 67 (1997) 69.
[16] D. Pavlov, J. Power Sources 53 (1995) 9.